JOURNAL OF APPLIED POLYMER SCIENCE VOL. 12, PP. 1009–1015 (1968)

Creep Behavior of Polyethylene Melts

TADAO KATAOKA, *Textile Research Institute of the Japanese Government, Kanagawaku, Yokohama, Japan*

Synopsis

Creep behavior of branched polyethylene melts with various molecular weight distributions are examined experimentally. The order of the steady-state compliance is in accord with the prediction from the molecular weight distribution. The shear rate dependence of viscosity and steady-state compliance are analyzed according to Pao's theory.

INTRODUCTION

The elastic effect of amorphous polymers is measured by various methods.[1] Creep behavior is one of the direct manifestations of the elastic effect and is observed principally by a relatively simple apparatus. In polymer melts, however, the contribution of flow in the creep experiment is much larger than that of the elastic effect, and the latter is sometimes masked by the former. Thus, creep data of great accuracy are difficult to obtain.

If the molecular parameters are known in detail, the steady-state compliance, for example, would be predicted from the theoretical considerations,[1–4] at least in the linear viscoelastic region. A quantitative prediction of steady-state compliance, however, requires accurate information about the higher average molecular weights,[1,4] which are difficult to obtain experimentally.

In this paper we describe the creep behavior of polyethylene melt. The main objectives of the study were, first, to obtain the steady-state compliance of samples with various molecular weight distribution and, second, to examine the effect of shear rate on steady-state compliance.

EXPERIMENTAL

Materials

The materials used are given in Table I; they were fractions, blends of fractions, and unfractionated polymers of branched polyethylene. Fractions were prepared by large-scale column fractionation[5] of sample Y, which was supplied by Mitsubishi Yuka Co. Ltd. The blend of fractions was prepared by precipitating the solution, which contained respective amounts of two fractions (YF3 and YF6) in the precipitant.

TABLE I
Critical Shear Stress, Viscosity, Steady-State Compliance, and $\bar{M}_{z+1}\bar{M}_z/\bar{M}_w^2$

Sample no.	Mol. wt.[a] $\bar{M}_w$ ($\times 10^{-5}$)	Crit. shear stress σ_c, dynes/cm.^{2} ($\times 10^{-4}$)	Viscy. η, poise ($\times 10^{-5}$)	Steady-state compl. J_e ($\times 10^5$)	$\bar{M}_{z+1}\bar{M}_z/\bar{M}_w^2$
Fractions[b]					
YF3	0.06	—	0.000125	—	—
YF6	1.7	0.9	20	1.7	7
YF9	1.8	1.0	22	1.6	6
YF12	2.0	1.2	30	1.8	6
Blends of fractions[c]					
B1	1.4	1.1	7.0	4.0	20
B3	1.0	0.3	3.0	6.0	38
Unfractionated polymers[d]					
Y	0.95	1.0	2.6	1.5	11
D1 (DYNF)	1.1	0.6	5.4	2.5	15
D2 (DYNH-1)	1.3	0.5	8.2	3.0	16
D3 (DYNH-3)	1.05	0.5	3.5	3.0	20
D4 (DYNJ)	2.0	0.4	28	3.6	14
D5 (DFD-6005)	2.2	0.5	36	6.4	20

[a] Weight-average molecular weights were calculated from the following relation:[6] $\log \eta = 3.4 \log \bar{M}_w + (3.16 \times 10^3/T) - 19.0$.

[b] Fractions were prepared from sample Y.

[c] Blended Samples were prepared by mixing YF3 and YF6, their ratios being about 1:2 and 2:1 for B1 and B3, respectively.

[d] Sample Y was supplied from Mitsubishi Yuka Co. Ltd.; samples D1 to D5 are Bakelite-type polyethylene.

Three types of molecular weight distribution are schematically shown in Figure 1, and for convenience they are denoted types I, II, and III. The molecular weight distribution of the blended sample B1 is approximated by type II; that of B3, by type III. From the fractionation results,[5] it was known that sample Y had a molecular weight distribution similar to type II.

Values of the weight-average molecular weight $\bar{M}_w$ given in column 2 of Table I are those calculated from the melt viscosity (η) data by means of the relation

$$\log \eta = 3.4 \log \bar{M}_w + (3.16 \times 10^3/T) - 19.0 \quad (1)$$

reported by Tung,[6] where T is the absolute temperature.

Apparatus

The apparatus used was a cone–plate viscometer operated at a constant shear stress. Two cones with the half-angle of 88° were used. One had

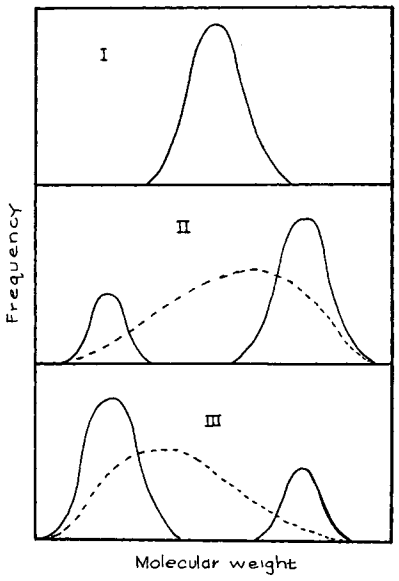

Fig. 1. Schematic representations of three types of molecular weight distribution.

a radius of 3 cm. and the other a radius of 1.5 cm.; the former was used throughout and the latter for obtaining results under high shear stress. The cone was fixed and the plate rotated on a pivot bearing. The friction due to the bearing was about 2.4 g.-cm. of torque, which corresponds to a shear stress of about 42 or 340 dynes/cm.^{2} for a cone 3 cm. or a 1.5 cm. in radius, respectively. The effective shear stress at the experimental run was calculated by subtracting this friction.

The rotation of the plate was measured by a lamp-and-scale method, in which a mirror was mounted on the plate shaft. The angle of rotation of the plate was converted to creep compliance $J(t)$. All experiments were carried out at 152°C. In all cases the steady state was reached within 1000 sec.

RESULTS AND DISCUSSION

Steady-State Compliance

In Figure 2 the creep compliances $J(t)$ for sample D-4 are plotted; they were determined at shear stress σ of 390 and 620 dynes/cm.^{2}, which correspond to shear rate $\dot{\gamma}$ under steady flow of 1.4×10^{-4} and 2.2×10^{-4} sec.$^{-1}$, respectively. The initial parts of the creep and recovery behavior are shown in somewhat enlarged scale. Within the experimental error the creep compliance $J(t)$ was determined uniquely as long as the shear stress was relatively low, and the curve of subtracted flow contribution agreed with the recovery curve. In other words, the linear relation between deformation or deformation rate and shear stress was preserved. With

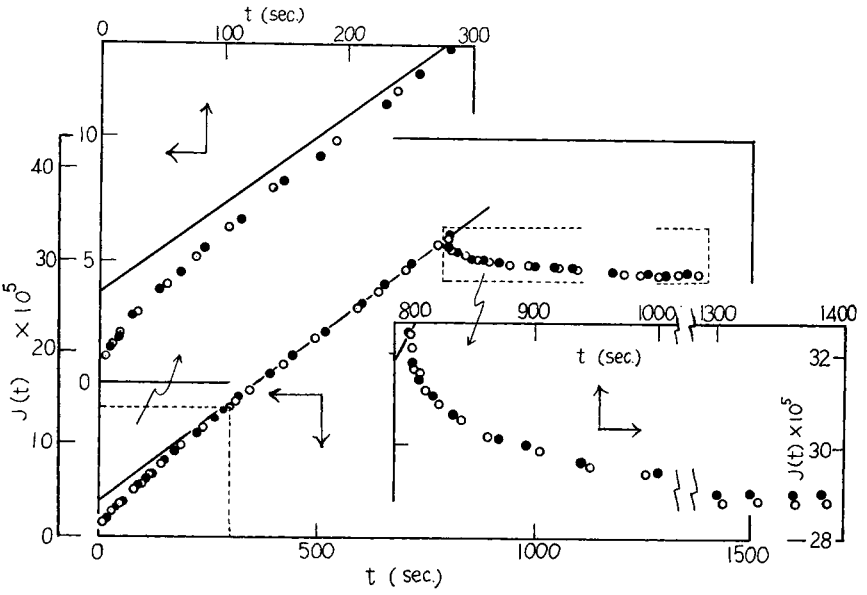

Fig. 2. Creep compliance $J(t)$ versus t for sample D-4. Shear stress σ and shear rate γ: (O) 390 dynes/cm.^{2} and 1.4 $\times$ 10^{-4} sec.$^{-1}$; (●) 620 dynes/cm.^{2} and 2.2 $\times$ 10^{-4} sec.$^{-1}$.

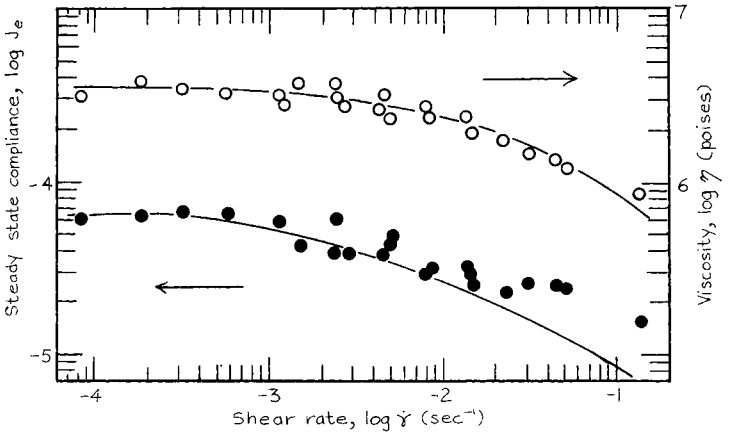

Fig. 3. Effect of shear rate on (O) viscosity and (●) steady-state compliance for sample D-5. Solid lines are those calculated from eqs. (3) and (4).

further increase in shear stress the linear relation failed (see Figs. 3 and 4). The magnitude of shear stress above which the linearity breaks was practically the same for viscosity η and steady-state compliance J_e. We denote the critical shear stress as σ_c and give it in column 3 of Table I.

NOTE: In this paper we denote shear stress as σ instead of the more conventional letter τ, because we use the letter τ as the retardation time. The value σ_c was defined as the shear stress at which η decreases about 10% from its zero shear value.

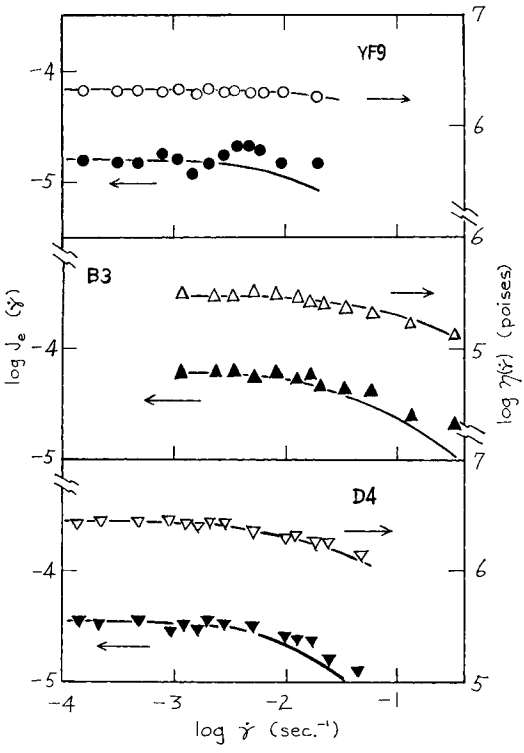

Fig. 4. Effect of shear rate on viscosity (open mark) and steady-state compliance (closed mark) for samples (○) YF9, (△) B3, and (▽) D4.

Table I summarizes the results for all samples. The values of η in column 4 and of J_e in column 5 are those obtained under relatively low shear stress and are considered to be zero shear values. The value of J_e for sample YF3 was not determined, because the flow contribution was too large to allow a reliable value of J_e. The value of J_e increases in the order of the type I, II, and III (in Fig. 1) of the molecular weight distribution.

The steady-state compliance J_e is a measure of the energy stored during the steady flow and depends greatly on the molecular weight distribution.[1,4,7] For polydisperse polymer it is given, from the Rouse theory, by

$$J_e = (2/5)\bar{M}_{z+1}\,\bar{M}_z/\bar{M}_w\,\rho\,RT \qquad (2)$$

where ρ is the density, R the gas constant, and $\bar{M}_z$ and $\bar{M}_{z+1}$ the z and $z+1$ average molecular weights. Using the value of J_e in Table I, we can calculate the value of $\bar{M}_{z+1}\bar{M}_z/\bar{M}_w$, from which the value $\bar{M}_{z+1}\bar{M}_z/\bar{M}_w{}^2$, a measure of the molecular weight distribution, was calculated. In column 6 of Table I are given the values. The value for fractions is about 6, which seems to be somewhat higher than what might be expected. The fractionation probably was not carried out effectively enough to fractionate

the higher molecular weight parts. The value of $\bar{M}_{z+1}\bar{M}_z/\bar{M}_w^2$ for sample Y is 11, which is somewhat lower than those of the other whole polymers. The low value for sample Y is in accord with the fact that its molecular weight distribution is similar to type II in Figure 1.

The value of σ_c given in column 3 of the table is about 10^4 dynes/cm.[2] for fractions and samples of type II distribution. This value is in accord with Ferry's suggestion (page 85 in ref. 1), but the values for the other samples are much smaller. The value of σ_c may also depend on the higher average molecular weights.

Effect of Shear Rate on Steady-State Compliance and Viscosity

Figure 3 shows the dependence of steady-state compliance J_e and viscosity η on shear rate $\dot{\gamma}$ for the sample D-5. Both $J_e(\dot{\gamma})$ and $\eta(\dot{\gamma})$ decrease with the increase in shear rate. Boyd[8] measured the shear rate dependence of η and J_e for solutions of poly(methyl methacrylate) in dibutyl phthalate and polyethylene melts and showed that Pao's theory[9] was applicable successfully to the results. Pao's hydrodynamic theory[9] formulated in terms of the retardation spectrum gives the following expressions:

$$J_e(t, \dot{\gamma}) = \sum_i J_i/(1 + \dot{\gamma}^2 \tau_i^2) \exp\left\{-t/\tau_i\right\} \tag{3}$$

$$1/\eta(\dot{\gamma}) = \frac{1}{\eta_0} + \sum_i (J_i/\tau_i)\left[\dot{\gamma}^2 \tau_i^2/(1 + \dot{\gamma}^2 \tau_i^2)\right] \tag{4}$$

where η_0 = zero shear viscosity, and J_i = contribution to compliance associated with retardation time τ_i. In this work, as in the work of Boyd,[8] a finite spectrum of retardation times was determined by the following method. The value of $\log J_R(t)$, the logarithm of recovery compliance, obtained at low shear stress, was plotted against t. A straight line was drawn through the points at the longest times. The longest retardation time τ_1 was found from the slope, and its contribution J_1 was determined from the intercept. Then $\log [J_R(t) - J_1 \exp\left\{-t/\tau_1\right\}]$ was plotted against t and τ_2 and J_2 were determined. The process was repeated until the entire curve was represented. Thus, we determined six constants for the sample D-5: $\tau_1 = 420$ sec., $J_1 = 3.8 \times 10^{-5}$; $\tau_2 = 49$ sec., $J_2 = 1.1 \times 10^{-5}$; and $\tau_3 = 7$ sec., $J_3 = 1.5 \times 10^{-5}$. By using these values $\eta(\dot{\gamma})$ and $J_e(\dot{\gamma})$ are calculated from eqs. (3) and (4); they are shown in Figure 3 as the solid lines. Agreement with experimental points is rather good. It is somewhat startling that the calculated $\eta(\dot{\gamma})$ represents the data points quite satisfactorily. The calculated $J_e(\dot{\gamma})$ decreases more rapidly with $\dot{\gamma}$ than the observed. The disagreement may be attributed to the poor experimental accuracy of the curve of $J(t)$ versus t, which makes it impossible to determine shorter retardation times, or to some systematic failure, which overestimates the value of J_e at high shear.

The data for three other samples are given in Figure 4, in which it is also shown that the agreement of the data points with the calculated curve is better for $\eta(\dot{\gamma})$ than for $J_e(\dot{\gamma})$.

Although the experimental accuracy is rather poor, particularly for $J_e(\dot{\gamma})$, and the range of data is not sufficiently broad, it may be accepted that Pao's theory is applicable to the present results.

References

1. J. D. Ferry, *Viscoelastic Properties of Polymers*, Wiley, New York, 1961.
2. P. E. Rouse, *J. Chem. Phys.*, **21**, 1272 (1953).
3. J. D. Ferry, *J. Appl. Phys.*, **26**, 359 (1955).
4. F. Bueche, *J. Appl. Phys.*, **26**, 738 (1955).
5. T. Kataoka, *Bull. Textile Res. Inst. (Japan)*, **64**, 71 (1963).
6. L. H. Tung, *J. Polymer Sci.*, **46**, 409 (1960).
7. H. Leaderman, R. G. Smith, and L. C. Williams, *J. Polymer Sci.*, **36**, 233 (1959).
8. R. H. Boyd, *J. Appl. Phys.*, **29**, 953 (1958).
9. Y. H. Pao, *J. Appl. Phys.*, **28**, 591 (1957).

Received July 3, 1967
Revised September 8, 1967